Heterogeneous nucleation of the primary phase in the rapid solidification of Al-4.5wt%Cu alloy droplet

A Maitre, A-A Bogno, Marie Bedel, G Reinhart, H Henein

Heterogeneous nucleation of the primary phase in the rapid solidification of Al-4.5wt%Cu alloy droplet

2015 IOP Conf. Ser.: Mater. Sci. Eng. 84 012013

(http://iopscience.iop.org/1757-899X/84/1/012013)

Heterogeneous nucleation of the primary phase in the rapid solidification of Al-4.5wt%Cu alloy droplet

A Maitre[1], A-A Bogno[1], M Bedel[2], G Reinhart[2] and H Henein[1]

1Department of Chemical and Materials Engineering, University of Alberta, Edmonton, AB, Canada
2Aix-Marseille University & CNRS, IM2NP UMR 7334, Campus Saint-Jérôme, Cas142, 13397 Marseille Cedex 20, France

Email: maitre@ualberta.ca

Abstract. This paper reports on rapid solidification of Al-Cu alloys. A heterogeneous nucleation/growth model coupled with a thermal model of a falling droplet through a stagnant gas was developed. The primary undercooling as well as the number of nucleation points was compared with Al-Cu alloy droplets produced by Impulse Atomization (IA). Based on experimental results from Neutron Diffraction, secondary (eutectic) phases were obtained. Then, primary and secondary undercoolings were estimated using the metastable extensions of solidus and liquidus lines calculated by Thermo-Calc. Moreover, Synchrotron X-ray micro-tomography has been performed on Al-4.5wt%Cu droplets. The undercoolings are in good agreement. Results also evidence the presence of one nucleation point and are in agreement with the experimental observations.

1. Introduction

Manufacturing of most metallic alloy products involves solidification at some stage. Mechanical properties of these products are generally related to their solidification microstructures. Depending on the final application of a product, a certain type of microstructure is more appropriate compared to another. For a product that requires directional properties, a microstructure of columnar grains is needed while isotropic properties are satisfied with an equiaxed structure. Generally, post-processing of the solidified materials is required to obtain the final product with desired properties. These post-solidification treatments are generally time-consuming and therefore increase the production cost without fully eliminating solidification related defects such as segregation. Therefore, it is important to understand all the dynamics involved in the formation of solidification microstructures in order to control the properties of the final products. As dendrites growth from an undercooled melt depends a great deal on the nucleation undercooling. Therefore, determination of undercooling and the resulting growth rate, recalescence, microsegregation/phase fraction and grain size is very important.

Al-Cu alloys (4.5, 5, 10 and 17 wt% Cu) have been produced by IA and the last three compositions were analysed in our previous papers [1, 2]. IA is a single fluid atomization technique that is capable of producing droplets of controlled size having a relatively narrow distribution and a predictable cooling rate. The alloys (350 to 450g) were melted in a graphite crucible by means of an induction furnace and atomized at 850ºC in an almost oxygen free chamber (10ppm) under Nitrogen, Helium or Argon atmospheres. The atomized droplets rapidly solidify during their fall by losing heat to the

stagnant atmosphere and are quenched in a collecting beaker filled with oil to avoid any solid-state reaction that could alter the microstructures. Subsequently, the solid droplets are washed, dried and sieved into different sizes. A detailed description of the IA process is given in [3]. A solidification model of a droplet falling through a stagnant gas, based on heterogeneous nucleation/growth was developed. The primary undercooling as well as the number of nuclei is considered and the results were compared to experimental results of a rapidly solidified Al-4.5 wt%Cu droplet, generated by IA.

2. Determination of the number of nuclei

2.1. Thermal model

For a hot spherical droplet moving in a cooler surrounding fluid, thermal energy is transferred within the droplet by conduction and between the surface of the droplet and the surrounding gas by forced convection, conduction and radiation. An equation describing the rate of heat energy lost at the droplet surface is given by:

$$q = h_{eff}\ A\left(T_m - T_\infty\right) \tag{1}$$

where h_{eff} is the effective heat transfer coefficient and consists of the additive contribution of convection, conduction and radiation heat transfer mechanisms. A is the surface area of the droplet, T_m is the droplet surface temperature and T_∞ is the free stream gas temperature (300 K). For alloys such as aluminum, the effective heat transfer for a moving droplet is dominated by convection. Radiation heat transfer can be significant for higher temperature alloy systems (iron based alloys).

One approach to quantify the convective component (h_c) of h_{eff} has been through the use of semi-empirical equations [4-10] in which the Nusselt number (Nu) is averaged over the entire droplet surface. The general form of these semi-empirical equations for calculating the effective heat transfer coefficient is

$$\mathrm{Nu} = \frac{H_C.D}{k_g} = A + B.\,\mathrm{Pr}^m\,.\,\mathrm{Re}^n \tag{2}$$

where D is the droplet diameter, $\mathrm{Re} = \dfrac{\rho_g.\nu.D}{\mu_g}$, $\mathrm{Pr} = \dfrac{C_p^g.\mu_g}{k_g}$, k_g, C_p^g, ϱ_g and μ_g are the conductivity, heat capacity, density and viscosity of the gas respectively and A, B, m and n are constants.
Considering the correlation proposed by Whitaker [3] and a correction term (due to the definition of Nu at Re=0) [11], equation (2) can be rewritten as

$$\mathrm{Nu} = \frac{H_C.D}{k_g} = 2.0\left(\frac{B}{k_s(\alpha+1)}\frac{T_s^{\alpha+1} - T_\infty^{\alpha+1}}{T_s - T_\infty}\right) + \left(0.4\,\mathrm{Re}^{1/2} + 0.06\,\mathrm{Re}^{2/3}\right)\mathrm{Pr}^{0.4}\left(\frac{\mu_\infty}{\mu_S}\right)^{1/4} \tag{3}$$

where k_s is the gas conductivity at the droplet surface temperature (T_s), B is the pre-power coefficient from the variation of the gas conductivity with temperature, α is the power coefficient in this same equation (Table 1) and $\dfrac{\mu_\infty}{\mu_s}$ is the ratio between the viscosity at the free stream gas temperature and the viscosity at the droplet surface temperature.

Table 1 – Thermophysical properties of nitrogen, helium and argon [12-14]

Property (all T values in K)	**Nitrogen**	**Helium**	**Argon**
Density (kg/m^3)	$335.55\ T^{-0.9971}$	$37.303\ T^{-0.9559}$	$539.23\ T^{-1.0205}$
Specific heat (J/kg.K)	$978 + 0.182\,T$	5197	520
Dynamic Viscosity (Pa.s)	$3.79\times10^{-7}\ T^{0.6766}$	$4.3679\times10^{-7}\ T^{0.6702}$	$2.38\times10^{-7}\ T^{0.6702}$
Conductivity (W/m.K)	$0.0344\times10^{-2}\ T^{0.7609}$	$0.2778\times10^{-2}\ T^{0.7025}$	$0.0186\times10^{-2}\ T^{0.7915}$

Several assumptions were made in the model formulation:
1 - Internal temperature gradients in droplets are negligible (Biot < 0.1 in the droplet size studied);
2 - The time for stream break up and spheroidization of ligaments emanating from the orifice plate is very small compared to the solidification time [15];
3 - The initial velocity of the droplet exiting the orifice is 0.5 m/s [16, 17];
4 - The ambient gas temperature remains constant during atomization;
5 - For radiation heat transfer, a droplet emissivity ε = 0.1 was used [18];
6 - Thermal interaction between droplets is negligible;
7 - Droplet diameter decreases during solidification.

Based on these assumptions, the governing heat transfer equation for droplet cooling is:

$$\frac{dT_m}{dt} = -\frac{6\,h_{eff}}{\rho_m.Cp_m.D}\left(T_m - T_\infty\right) \tag{4}$$

where $\frac{dT_m}{dt}$ is the change in droplet temperature with time, ϱ_m and Cp_m are the droplet density and specific heat, respectively. The h_{eff} term used in Equation (4) was calculated using a linearized radiation term and h_c calculated with Equation (3). During solidification, an effective Cp_m (in Equation (4)) was calculated as

$$Cp_m = \frac{dH}{dT_m} = \frac{df_s}{dT_m}.\Delta H_f + Cp \tag{5}$$

where *fs* is the fraction solid at temperature T_m and ΔH_f is the latent heat of fusion. The equation (4) is solved using a fourth order Runge-Kutta method. More details can be found in [11].

2.2. Nucleation model

This model considers a heterogeneous nucleation with growth in the frame of a cellular method. The start temperature is taken just below the liquidus temperature. At each step the temperature is determined using equation (4) and the critical radius r^* as well as the corresponding energy ΔG^* related to the formation of a nucleus at this temperature are calculated using equation (6) to (8)

$$r^* = \frac{2\gamma T_L}{\Delta H_f \Delta T} \tag{6}$$

$$\Delta G^* = \frac{16\pi\gamma^3 T_L^2}{3\Delta H_f^2 \Delta T^2} f(\theta) \tag{7}$$

$$f(\theta) = \frac{(1-\cos(\theta))^2 . (\cos(\theta)+2)}{4} \tag{8}$$

where γ is the surface energy, T_L is the liquidus temperature, ΔT is the primary phase undercooling and θ is the wetting angle.

It is then possible to determine the nucleation rate $I_F(T)$ (9) and the nuclei density $n(T)$ (10). The probability density function $P(T)$ (11) for the nucleation of the droplet and the probability $P_m(T)$ for a mesh to become a cluster can be determined as well

$$I_F(T) = 10^{30} \times e^{\left(\frac{-\Delta G^*}{kT}\right)} \tag{9}$$

$$n(T) = \int_{T(t)}^{T(t+\delta t)} \frac{I_F(T)}{Q} dT \tag{10}$$

$$P(T) = \frac{I_F(T) V_{droplet}}{Q} \exp\left(-n(T) V_{droplet}\right) \tag{11}$$

$$P_m(T) = \frac{\left[n(T(t+\delta t)) - n(T(t))\right] V_{droplet}}{x_{mesh}} \tag{12}$$

x_{mesh} is the number of mesh in the system and $V_{droplet}$ is the volume of the considered droplet. At each step, r^*, ΔG^* and so $P(T)$ and $P_m(T)$ are calculated. The model used is partially stochastic as a random number is taken and compared to the probabilities and can be divided in two parts ($P(T)$ for the nucleation start and $P_m(T)$ for the number of clusters). Firstly, a random number is compared to $P(T)$ at each step, if the number is lower than $P(T)$ then nucleation starts. This provides us the nucleation temperature (T_L-ΔT) and so the undercooling. In a second time and only if the nucleation is allowed, a run is done on the meshes contained in the droplet (due to memory issue, only a box of 10×10×10 μm^3 is considered for the number of clusters and not for the entire droplet). All the meshes are investigated. Each time, a different random number is selected and compared to $P_m(T)$. If this number is higher than $P_m(T)$, the mesh will stay liquid otherwise it will become a cluster. It should be noted that a homogeneous nucleation model has been attempted. Due to a too small value of I_F (i.e. too "important" value of ΔG^*) no nucleation was observed.

2.3. Growth model

During the growth process, the radius of each cluster is updated for each step by using

$$r(t+\delta t) = r(t) + v.\delta t \qquad (13)$$
$$r(t=0) = r^*$$

where v is the growth velocity determined by the LKT model [19] (Figure 1). It was assumed that the first introduced cluster will be the first to grow and other clusters will follow. Each time the size of a cluster is updated using eq (12), the temperature of the whole droplet, using eq (4), is determined. If the temperature of the droplet becomes higher than the temperature required for the stability of some clusters, these clusters are then re-melted. Thus a distinction exists between the number of determined clusters and the number of nuclei (clusters which do not re-melt).

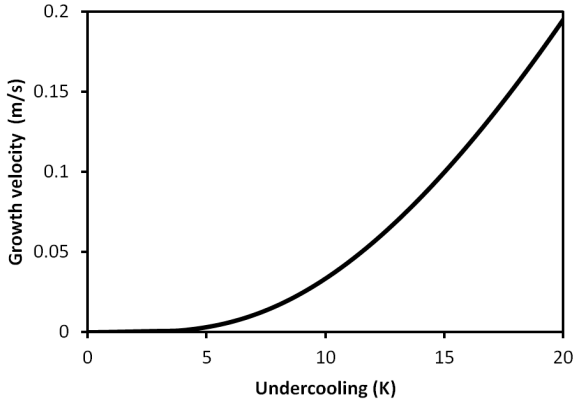

Figure 1: Evolution of the growth velocity for Al-4.5wt%Cu with the primary undercooling.

3. Results and discussions

Al-4.5wt Cu droplets of different sizes were obtained by IA under Ar and He. This work focuses on a droplet with average size (diameter) of 196 µm atomized in He (data used for the model are summarize in Table 2).

Table 2 – Properties of the Al-4.5wt%Cu alloy under investigation

gas	C_p^l ($J.m^{-3}K^{-1}$)	ΔH_f ($J.m^{-3}$)	T_m (K)	θ (°)	Diameter (μm)	γ (J/m^2)	Q (K/s)	Growth velocity (m/s)
He	3.25×10^6	1.07×10^9*	920	23	196	0.093*	5650	0.044

* A. Roosz, E.Halder and H. E. Exner, Mater. Sci. Tech., 1986, vol. 2, pp. 1149-1155

Using the model described in the previous section, the primary dendritic nucleation undercooling is predicted to be 11K for the investigated droplet, a value that is in good agreement with the experimentally obtained value of 10.9K±3(error inherent to experimental measurements). Indeed, experimentally the primary dendritic nucleation undercooling is obtained by combining semi-empirical coarsening models of secondary dendrite arms spacing with the eutectic nucleation undercooling estimated through the measurement of eutectic fraction within the investigated droplet microstructure by Rietveld refinement analysis of neutrons diffraction data. The eutectic fraction is estimated by extending the solidus and liquidus lines of the Al-rich corner of Al-Cu phase diagram using Thermo-Calc. A detailed description of this analysis is given in [1, 2]. However, it is worth

noting that the time/temperature variation of the coarsening parameter was not taken into account in [1, 2] whereas this variation is considered in the present case.
Figure 2 shows the number of clusters distribution (modelling was performed for 30 different seeds). The number of clusters introduced in the 10×10×10 μm^3 box varies between two and ten (depending on the seed number of the random number generator) with an average of six clusters.

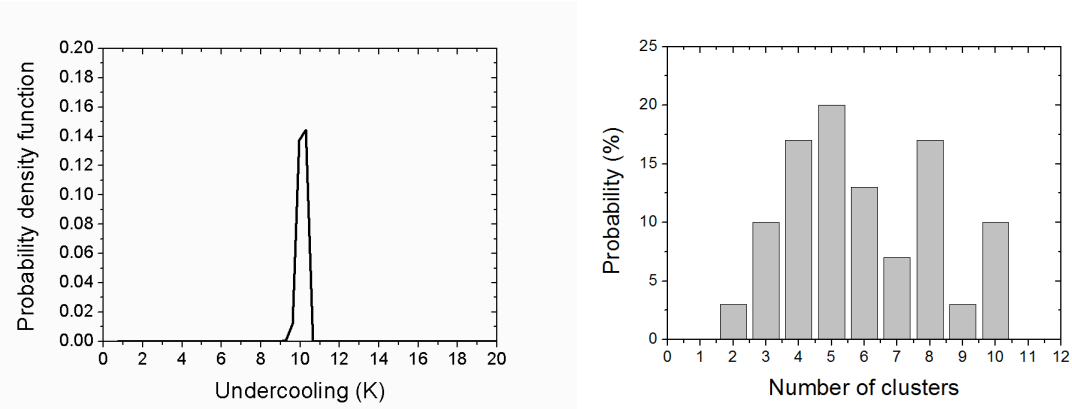

Figure 2: Probability density function for the considered droplet (a) and distribution of the number of clusters (b) (performed for 30 seeds of the random number generator).

When the first step of growth occurred, the solid fraction formed during the growth of the first cluster leads to a sufficient increase in the temperature of the whole droplet (recalescence) that the other clusters become unstable. As the temperature is calculated for the entire droplet and not only for the 10×10×10 μm^3 in size box, this means that the other clusters being introduced in the droplet will re-melt. This results in the presence of only one nucleus. The model was run for a droplet with average of 925 µm as well as for a droplet atomized in N_2 and the same trend was observed.

Synchrotron X-ray micro-tomography has been performed on several (99) Al-4.5wt%Cu alloy droplets with sizes ranging from 100 to 355 μm atomized under He [20]. The image acquisition and the 3D reconstructions were carried-out on the ID19 beamline of the ESRF (European Synchrotron Radiation Facility). A series of X-ray images with contrast due to the density and composition difference between the primary α-Al phase which appears in dark grey and the eutectic (α-Al+θ-Al_2Cu) which appears in light grey and the porosity appearing as black areas within the droplet. These images obtained at different view angles were then reconstructed into 3D droplet microstructures. Such 3D reconstructions of the inner structure of the droplets enabled us to locate the nucleation position by determining the intersection of the primary arms of the dendritic structure. A typical image obtained with synchrotron X-ray micro-tomography is given in Figure 3. The slice in the droplet is chosen in this figure in such a way that the nucleation centre can be clearly visualized. This work highlighted the presence of only one nucleus in 95 droplets out of the 99 droplets visualized. In the 4 other droplets, only 2 nuclei were observed. These experimental observations are in agreement with our model prediction.

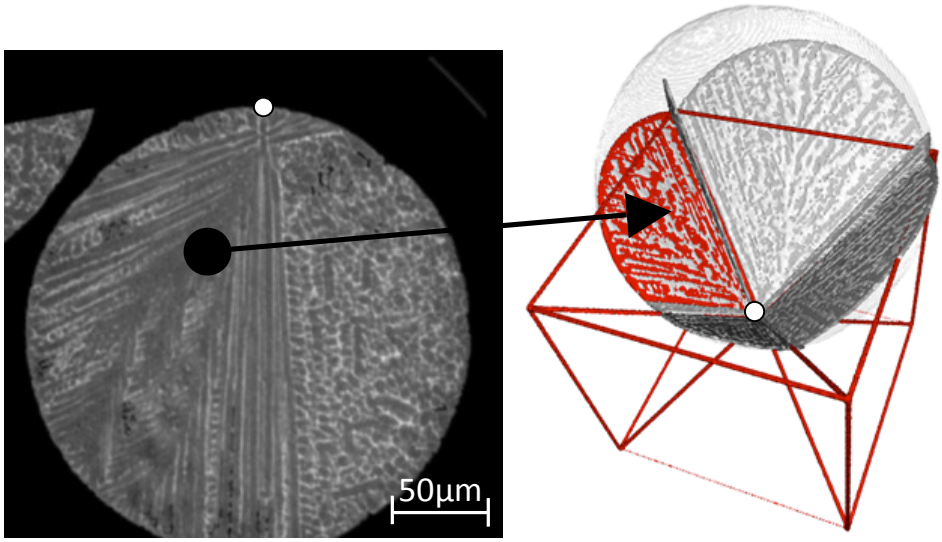

(a) (b)

Figure 3: Synchrotron X-ray micro-tomography result showing (a) a droplet cross-section and (b) the corresponding 3D-reconstruction with characteristic planes and the position of the nucleation centre (white dot) in a 290 μm diameter Al-4.5wt%Cu droplet atomized in helium.

4. Conclusions

Primary dendritic nucleation undercooling of an IA Al-4.5wt%Cu droplet is investigated. A numerical prediction of the primary dendritic nucleation undercooling was achieved based on a thermal model coupled with a heterogeneous nucleation/growth model of a droplet falling through a stagnant gas. The model prediction is compared with experimental results of primary dendritic nucleation undercooling estimated using a metastable extension of solidus and liquidus lines of the phase diagram by Thermo-Calc and a semi-empirical coarsening model of secondary dendrite arms spacing. The comparison yields a good agreement between the experimental result and the model prediction of primary dendritic nucleation undercooling of the investigated droplet. Furthermore, the number of nuclei in the droplet was numerically analysed. It appears that only one nucleus is expected to form, a results that is confirmed by the evidence of a single nucleation point on 3D images of IA droplets obtained by synchrotron X-ray micro-tomography analysis

5. Acknowledgements

The authors are grateful to the Natural Sciences and Engineering Research Council of Canada (NSERC), the Canadian Space Agency (CSA), the European Space Agency (ESA) and the Agency National de Recherche (ANR-France) for their financial support. Dr. Jonas Valloton is also acknowledged for fruitful discussions.

References

[1] Herlach D M Galenko P and Holland-Moritz D 2007 *Metastable Solids from Undercooled Melts* (Oxford Pergamon Materials Series Elsevier)
[2] Bogno A, Delshad Khatibi P, Henein H and Gandin Ch-A 2014 *Under review in Met. Trans.*
[3] Bogno A, Khatibi P D, Henein H and Gandin Ch-A 2013 *Light Metals for Transportation*, (MS&T 2013)
[4] Ranz W E and Marshall W R Jr 1952 *Chem. Eng. Progress* **48**(3) 141-146
[5] Whitaker S 1972 *AIChE Journal* **18**(2) 361-371
[6] White F M 1974 Viscous Fluid Flow *McGraw-Hill Book Co., New York, NY* 213
[7] Vilet G C and Leppert G 1961 *Journal of Heat Transfer* **5** 163-175

[8] Jackson J D and Hatchman J C 1999 *Proc. Instn. Mech. Engrs.* **213A** 45-56
[9] Sayegh N N and Gauvin W H 1979 *AIChE Journal* **25**(3) 522-534
[10] Kramer H 1946 *Physica* XII **2-3** 61-80
[11] Wiskel J B, Henein H and Maire E 2002 *Can. Metall. Quart* **41**(1) 97-110
[12] Yule A J and Dunkley J J 1994 *Atomization of Melts: For Powder Production and Spray Deposition* (Claredon Press, Oxford, England) 28432
[13] Welty J R, Wicks C E and Wilson R E 1984 *Fundamentals of Momentum, Heat and mass Transfer* (3rd ed) (New York: John Wiley and Sons) pp 759
[14] Weast 1980 *CRC Handbook of Chemistry and Physics* (61th ed) (CRC Press inc. Boca Raton) pp D62, E2-E3
[15] Rabinovich V A Nedostup V I, Vasserman A A and Veksler L S 1988 *Thermophysical Properties of Neon, Argon, Krypton and Xenon* (10th ed) (USSR) pp 384-385, 417-418, 423-424
[16] Yuan D 1998 *Ph.D. Thesis, University of Alberta*
[17] Wiskel J B and Henein H 1999 *Proceedings of Fluid Flow Phenomena in Metals Processing* eds. El-Kaddah N, Robertson D G C, Johansen S T and Voller V R, TMS, (Warrendale) 517-524
[18] Kreith F 1973 *Principles of Heat Transfer* (3rd ed) (New York: Harper and Row) pp 236, 316-317, 339
[19] Galenko P K and Danilov D A 1997 *Physics Letter*s A **235** 271-280
[20] Bedel M Reinhart G Bogno A Nguyen-Thi H Boller E Gandin Ch-A and Henein H 2014 being published *IOP Conf. Ser. Mater. Sci. Eng.*